

PHARMACOKINETICS

Model-based evaluation of pulmonary pharmacokinetics in asthmatic and COPD patients after oral olodaterol inhalation

Correspondence Charlotte Kloft, Freie Universität Berlin, Institute of Pharmacy, Department of Clinical Pharmacy and Biochemistry, Kelchstr. 31, 12169 Berlin, Germany. Tel.: +49 (30) 8385 0676; Fax: +49 (30) 8384 50656; E-mail: charlotte.kloft@fu-berlin.de

Received 16 December 2015; **revised** 8 April 2016; **accepted** 28 April 2016

Jens Markus Borghardt^{1,2}, Benjamin Weber², Alexander Staab², Christina Kunz² and Charlotte Kloft¹

¹Institute of Pharmacy, Department of Clinical Pharmacy and Biochemistry, Freie Universität Berlin, 12169 Berlin, Germany and ²Translational Medicine and Clinical Pharmacology, Boehringer Ingelheim Pharma GmbH & Co. KG, Biberach, Germany

Keywords asthma, COPD, olodaterol inhalation, pharmacometrics, population pharmacokinetics, pulmonary absorption

AIMS

Olodaterol is an orally inhaled β_2 -agonist for treatment of chronic obstructive pulmonary disease (COPD). The aims of this population pharmacokinetic (PK) analysis were: (1) to investigate systemic PK and thereby make inferences about pulmonary PK in asthmatic patients, COPD patients and healthy volunteers, and (2) to assess whether differences in pulmonary efficacy might be expected based on pulmonary PK characteristics.

METHODS

Plasma and urine data after olodaterol inhalation were available from six clinical trials comprising 710 patients and healthy volunteers (single and multiple dosing). To investigate the relevance of covariates, full fixed-effect modelling was applied based on a previously developed healthy volunteer systemic disposition model.

RESULTS

A pulmonary model with three parallel absorption processes best described PK after inhalation in patients. The pulmonary bioavailable fraction (PBIO) was 48.7% (46.1–51.3%, 95% confidence interval) in asthma, and 53.6% (51.1–56.2%) in COPD. In asthma 87.2% (85.4–88.8%) of PBIO was slowly absorbed with an absorption half-life of 18.5 h (16.3–21.4 h), whereas in COPD 80.1% (78.0–82.2%) was absorbed with a half-life of 37.8 h (31.1–47.8 h). In healthy volunteers absorption was faster, with a half-life of 18.5 h (16.3–21.4 h) of the slowest absorbed process, which characterized 74.6% (69.1–80.2%) of PBIO.

CONCLUSIONS

The modelling approach successfully described data after olodaterol inhalation in patients and healthy volunteers. Slow pulmonary absorption was demonstrated both in asthma and COPD. Absorption characteristics after olodaterol inhalation indicated even more beneficial lung targeting in patients compared to healthy volunteers.

WHAT IS ALREADY KNOWN ABOUT THIS SUBJECT

- A long pulmonary residence time was demonstrated in healthy volunteers that might contribute to the long-lasting pulmonary efficacy of olodaterol inhaled with the Respimat® device.

- Altered airway characteristics in asthmatic and COPD patients can influence pulmonary pharmacokinetics and may thereby be relevant for pulmonary efficacy of inhaled drugs.

WHAT THIS STUDY ADDS

- This is the first published pharmacokinetic-based analysis quantifying the pulmonary fate of inhaled olodaterol in asthmatic and COPD patients.
- Slow absorption characteristics were demonstrated in asthmatic and COPD patients. An even more beneficial lung targeting in patients is anticipated compared to healthy volunteers.

Introduction

Oral inhalation is the preferred route of drug administration for the treatment of pulmonary diseases such as bronchial asthma or chronic obstructive pulmonary disease (COPD) [1, 2]. The rationale is a higher pulmonary efficacy and at the same time lower systemic exposure leading to better (systemic) safety profile compared to other routes of drug administration (e.g., oral). These advantages result from the drug being delivered directly to the effect site, i.e. the lungs, by oral drug inhalation. Subsequently, drug deposited in the lungs remains there until being absorbed to plasma or cleared from the airways (e.g., by mucociliary clearance). This means that both the amount of drug reaching the effect site and the pulmonary residence time might affect drug efficacy and safety [3–6].

For olodaterol, a once-daily inhaled β_2 -sympathomimetic drug for maintenance treatment of COPD inhaled with the Respimat® device, it was demonstrated by population modelling of healthy volunteer PK data that a pulmonary bioavailable fraction (PBIO) of approximately 50% of the nominal dose was absorbed by three parallel absorption processes (slow, intermediate and fast) [6]. The pulmonary absorption of the highest proportion (~70%) of the PBIO was characterized by an absorption half-life of 21.8 h, representing a long pulmonary residence time. This, in addition to the slow receptor off-kinetics of olodaterol [7], was regarded as contributing to its long-lasting local pulmonary efficacy [6].

However, the quantified pulmonary PK characteristics for inhaled olodaterol in healthy volunteers have not yet been evaluated for patients. The latter have altered airway characteristics such as narrowed airways in asthmatic and COPD patients [8] or an increased residual volume combined with a smaller pulmonary surface area in COPD potentially caused by emphysema [9]. As a result, altered pulmonary deposition patterns and/or pulmonary PK properties were demonstrated in patients [8]. Limitations of previous PK-based comparisons between healthy volunteers and patients were the small numbers of patients or the absence of data following intravenous (IV) administration, so that analyses were performed based solely on PK data after inhalation [10, 11]. However, without available IV data, the pulmonary PK cannot be evaluated independently from systemic drug disposition, i.e. the pulmonary bioavailable fraction and the pulmonary residence time cannot be determined.

Mathematical (pharmacometric) modelling can be applied to draw conclusions about the pulmonary fate of inhaled olodaterol in the target patient population by evaluating PK data from multiple clinical trials following different routes of administration (IV, inhalation, oral) [5, 6, 12–14].

Furthermore, it is possible to investigate whether differences in PK between patients and healthy volunteers can be attributed to subject-specific factors other than the underlying disease, such as age or smoking status [15]. Thus, the objective of this population PK analysis was to establish whether or not asthmatic or COPD patients demonstrate differing pulmonary PK characteristics from healthy volunteers, and also to evaluate whether differing drug efficacy in these subject groups might be expected based on PK characteristics after oral inhalation treatment with olodaterol.

Materials and methods

Data for PK model development

Olodaterol concentration data above the lower limit of quantitation (LLOQ) were available from a total of 6603 plasma and 2382 urine samples. These plasma and urine data were available from two Phase I (healthy volunteers) and four Phase II (patients) clinical trials after drug inhalation for PK model development and subsequent model evaluation. Overall, the clinical trials comprised one single dose (SD) and one multiple dose (MD) trial in each of healthy volunteers, patients with asthma, and patients with COPD (see Figure 1). In all clinical trials, olodaterol was inhaled as a solution via multiple puffs with the Respimat® Soft Mist™ inhaler. Table 1 provides an overview of the trials and evaluated PK data characteristics and the subject-specific factors. All trials were approved by the respective independent ethics committees, and were conducted in accordance with the Declaration of Helsinki and Good Clinical Practice guidelines. All healthy volunteers and patients provided written informed consent before trial inclusion. In-study validation at three nominal concentrations in all clinical trials demonstrated assay accuracy (relative recovery from target concentrations) ranging from 92.3% to 109.3% for plasma and 92.7% to 105.5% for urine, imprecision (% CV) ranged from 1.7% to 9.9% for plasma and 1.7% to 8.2% for urine. More specific details on the trial design can be found under the ClinicalTrials.gov identifiers: SD healthy volunteers, NCT02171780; MD healthy volunteers, NCT02171806; SD patients with asthma, NCT00928668; MD patients with asthma, NCT00467740; SD patients with COPD, NCT01809262; MD patients with COPD, NCT00452400.

Model development

Model development was performed using a stepwise approach. A previously developed systemic PK model based on healthy volunteer IV data [6] was assumed to describe

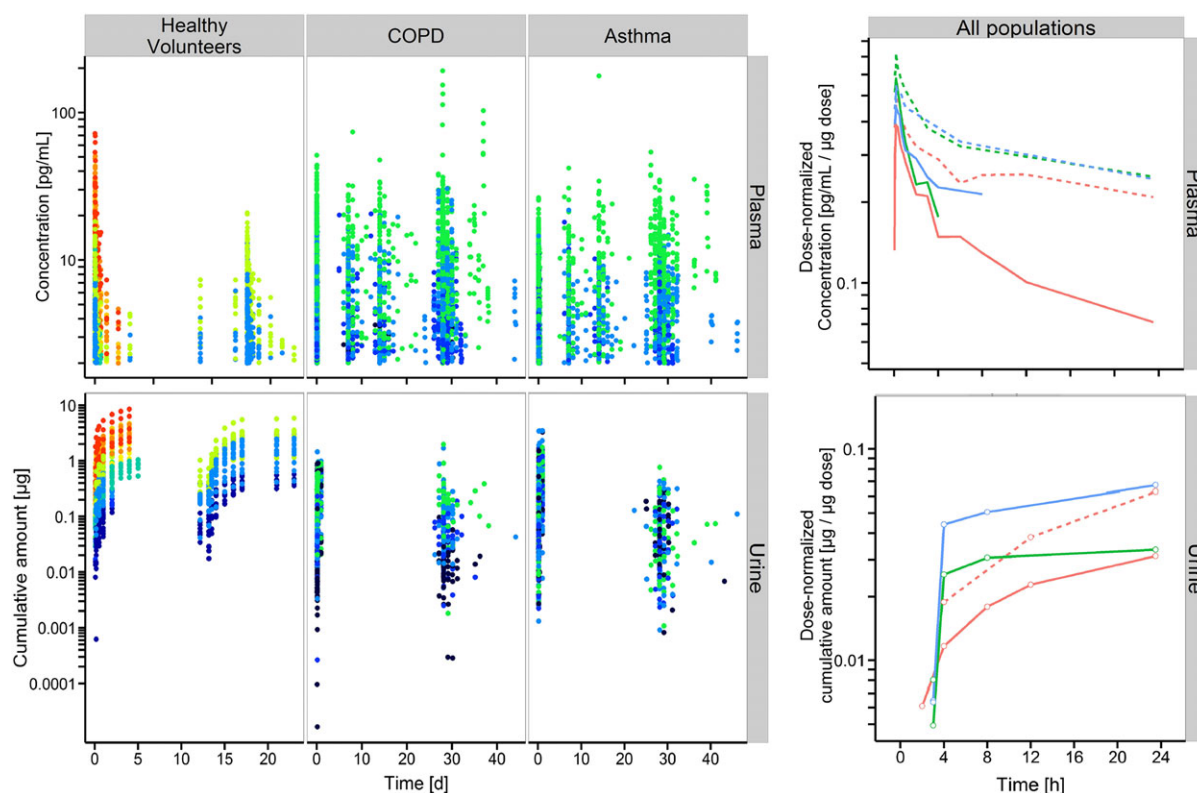


Figure 1

Observed data used for PK model development. Olodaterol plasma concentrations (upper panels) and cumulative amount excreted in urine (lower panels). Left panels: concentration/amounts vs. time after the first oral olodaterol inhalation with the Respimat[®] Soft Mist[™] inhaler, stratified by population (healthy volunteers, patients with COPD and patients with asthma). Urine collection was restarted with every orally inhaled olodaterol dose. Colour coding: Dose: ● 2 ● 2.5 ● 5 ● 10 ● 15 ● 20 ● 30 ● 40 ● 50 ● 60 ● 70. Right panels: median dose-normalized concentration–time or amount–time profiles after single dose (solid lines) and at steady state (dashed lines) for healthy volunteers (red lines), asthmatic patients (blue lines) and COPD patients (green lines). For better graphical illustration, data from 24 h after the inhaled dose are not shown. At steady state for asthma and COPD, only a single urine collection was performed, so that these amount–time profiles are missing. PK data in healthy volunteers were already published [6], but are presented in the same manner to facilitate comparison with patients

systemic disposition kinetics as a reference for healthy volunteers and patients. The relevance and potential limitations of this assumption are debated in the Discussion section. Hence, systemic olodaterol disposition PK and the associated between-subject variability (BSV) parameters were fixed for model development. Gastrointestinal absorption of swallowed drug was assumed to be negligible owing to low oral systemic availability of olodaterol [6]. The second part of the model, describing the pulmonary PK, was estimated based on plasma and urine concentration data after oral inhalation of olodaterol. Data below the LLOQ were not evaluated. Urine data were used additionally to define the terminal phase of olodaterol elimination, because it was found previously that urine concentrations remained above the LLOQ up to later time points than was the case for plasma [6].

Based on pooled PK data from all six clinical trials (healthy, asthma and COPD), the PBIO was estimated on a logit scale and was therefore constrained to lie between 0 and 1. In addition to three parallel pulmonary absorption processes (healthy volunteer reference model), two parallel and four parallel absorption processes were investigated as alternative pulmonary absorption model structures. Absorption processes were characterized by a first-order

absorption rate constant and a proportionality factor (constrained between 0 and 1) to quantify the proportion of the PBIO associated with the specific absorption process (see Figure 2). The number of estimated proportionality factors was $n - 1$, where n was the number of investigated parallel absorption processes. The remaining proportion of the last absorption process was calculated based on the other proportions so that the sum of all n proportions was equal to 1 (see Figure 2).

The second step of model development was to investigate the random effects model by stepwise inclusion of BSV components on pulmonary PK parameters. Both variance and covariance elements of the BSV parameter matrix were investigated and evaluated. Afterwards, between-occasion variability (BOV) was investigated on pulmonary PK parameters with BSV associated.

The last step of model development was the investigation of covariate–parameter relations based on a full fixed-effects modelling approach (FFEM) [16]. Covariate effects included in the FFEM were preselected based on physiological plausibility and comprised asthma and COPD as categorical covariates (see listed covariate–parameter relations in Table 2 for more details). Preselected covariate effects were investigated on all PK parameters for which a BSV parameter was

Table 1

Trial and baseline demographic characteristics of healthy volunteers, patients with asthma, and patients with COPD with PK data used for the population PK analysis

	All	Healthy	Asthma	COPD
Route of administration	Inhalation	Inhalation	Inhalation	Inhalation
Dosing	Single + multiple	Single + multiple	Single + multiple	Single + multiple
Administered doses with PK data [μg]	2–70	2.5, 5, 10, 15, 20, 30, 40, 50, 60, 70	2, 5, 10, 20	2, 5, 10, 20
Number of healthy volunteers/patients with PK data	710 (115 + 595)	101 (65 + 36)	271 (32 + 239)	338 (18 + 320)
Plasma PK data points above LLOQ used for analyses	$n = 6603$ TAD: 0:01 to 96:00 h	$n = 1152$ TAD: 0:02 to 96:00 h	$n = 2410$ TAD: 0:01 to 24:44 h	$n = 3041$ TAD: 0:01 to 25:28 h
Fraction of plasma PK data points below the LLOQ (2 pg ml^{-1}), %	38.1	46.2	38.5	34.2
Urine PK data points above LLOQ used for analyses	$n = 2382$ TAD: 1:01 to 240:18 h	$n = 858$ TAD: 2:00 to 240:18 h *	$n = 775$ TAD: 2.06 to 24:53 h *	$n = 749$ TAD: 1:37 to 24:20 h *
Fraction of urine PK data points below the LLOQ (10 pg ml^{-1}), %	3.21	3.21	3.37	3.23
Sex (male), %	58.2	85.1	44.3	61.2
Smoking status (non-smoker/ex-smoker/smoker), %	36.6 / 35.5 / 27.9	57.4 / 17.8 / 24.8	74.5 / 20.7 / 4.80	0 / 52.7 / 47.3
Ethnicity (Asian/Black/Caucasian), %	1.97 / 5.92 / 92.1	0 / 0 / 100	4.80 / 7.38 / 87.8	0.296 / 6.51 / 93.2
Age (median, range) [years]	53 (18–86)	34 (22–49)	43 (18–79)	64 (40–86)
BSA (median, range) [m^2]	1.89 (1.38–2.58)	1.99 (1.55–2.31)	1.85 (1.40–2.54)	1.89 (1.38–2.58)
Body weight (median, range) [kg]	77 (42–157)	81 (53–105)	75 (43–145)	77 (42–157)
Body height (median, range) [cm]	170 (147–201)	179 (157–194)	169 (147–196)	170 (150–201)
Creatinine clearance [ml min^{-1}][†]	93.5 (39.2–271)	116 (77.4–170)	100 (49.7–270)	78.9 (39.2–271)

*Time after dose for urine samples describe the end time of urine collections. †Creatinine clearance values were calculated according the Cockcroft-Gault-equation [29]. BSA: body surface area; IV: intravenous; LLOQ: lower limit of quantification; PK: pharmacokinetics; TAD: time after dose [hh:mm].

identified in the previous random-effects model development. Covariate effects on logit scale PK parameters were added to the transformed PK parameter, whereas covariate effects on other PK parameters (e.g., absorption rate constants) were implemented as a fractional change (see model code in the online supplementary material).

Starting with a FFEM that included all predefined covariate–parameter relations (see Table 2), the number of covariate–parameter relations was reduced in a subsequent model reduction process. When the magnitude of a covariate effect was small (<10% change in the specific PK parameter for the extreme covariate values in all studied populations) and the imprecision of a covariate–parameter relation estimate was high (relative standard error larger than 50%, based on the NONMEM variance–covariance matrix), the respective relationship was removed.

Model selection and evaluation for all steps was based on numerical and graphical criteria. The numerical criteria comprised objective function value (OFV), significant digits of the parameter estimates, relative standard errors based on the NONMEM variance–covariance matrix, and condition

number. The graphical goodness-of-fit (GOF) criteria comprised visual predictive checks (VPC) and standard GOF plots. Model development and simulations for VPC creation were performed with NONMEM 7.2 (Icon Development Solutions, Ellicott City, MD, USA) and PsN (Perl speaks NONMEM [17]). VPC visualization and post processing were performed with R 3.0.3. [18].

Model-based simulations

The magnitude of the effects of covariates on PK characteristics including model parameter imprecision was evaluated in the form of model-based simulations. For this reason, the influence of the identified covariates on PK metrics was quantified. PK metrics comprised the maximum plasma concentration (C_{max}), area under the plasma concentration–time curve (AUC_{plasma}) and area under the unabsorbed amount–time curve (AUC_{Lung}) after single dose (SD) and at steady state (SS, assumed after 14 doses of 5 μg). From the full NONMEM variance–covariance matrix, 1000 parameter sets were drawn for each investigated covariate effect (e.g., 1000 smokers or 1000 Asians) and used as input to simulate the PK metrics.

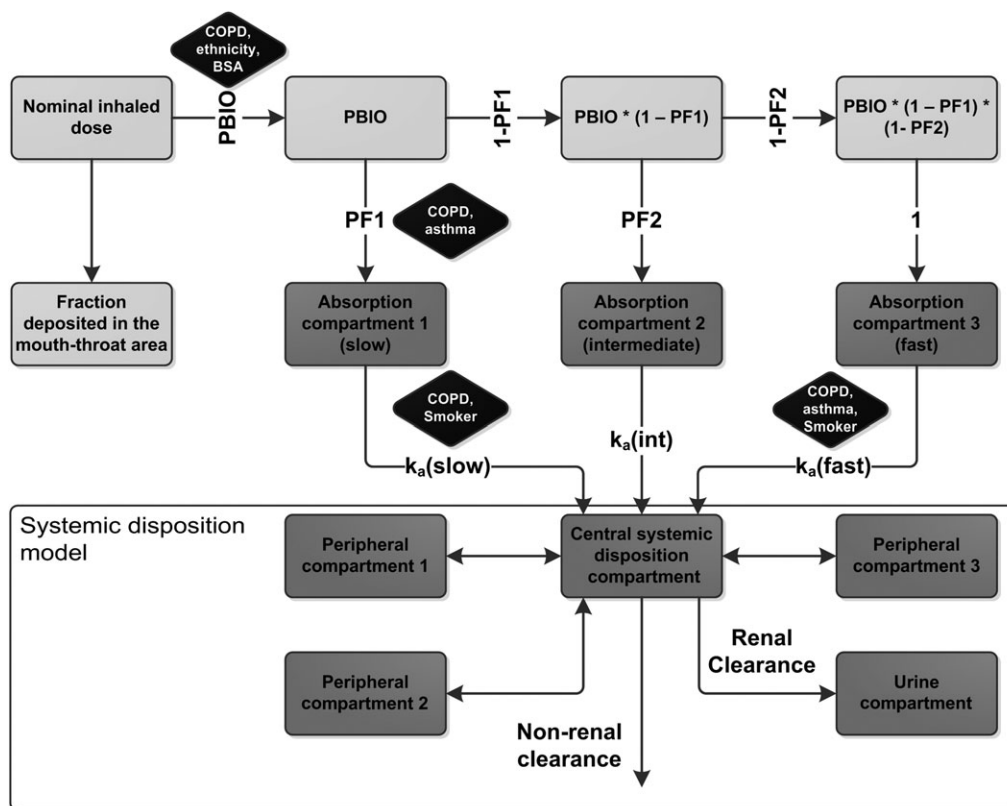


Figure 2

Population PK model developed based on pooled data from healthy volunteers, patients with asthma and patients with COPD. Dark grey compartments represent actual compartments of the model with mass transfer. The model can be separated into the systemic disposition model (lower part, based on intravenous data of healthy volunteers), and the pulmonary absorption part (upper part, developed based on additional inhalation data). Light grey compartments represent equations to calculate input to the absorption compartments. Black boxes display the statistically significant covariates. k_a : absorption rate constant, PBIO: pulmonary bioavailable fraction, PF: proportionality factor

Besides the univariate investigation of covariates, a covariate combination was investigated that accounted for all significant covariate–parameter relations that increased PBIO and influenced absorption half-lives. This was defined as the “highest lung disposition” scenario. In a post-processing step, simulated C_{max} and AUC metrics were normalized by the respective median simulated PK metric for a standard healthy volunteer (body surface area (BSA) of 1.89 m², non-smoker, Caucasian). To evaluate the magnitude of the covariate effect, the 95% confidence interval (CI) of the normalized ratios was calculated (two-sided).

To evaluate the magnitude of the identified covariate effects in the presence of overall (remaining unexplained) PK variability, the developed PK model was applied for a second model-based simulation. This simulation accounted for BSV and BOV, but did not implement the imprecision of the estimated parameters. From the full covariance matrix of random effects for BSV and BOV (NONMEM OMEGA matrix), 1000 parameter sets were drawn for each investigated covariate, as well as the above defined “highest lung disposition” scenario. Based on these parameter sets, the above defined PK metrics were simulated and compared to show (dis-)similarity in PK due to the influence of disease and other covariates. All simulations were performed in R 3.0.3 applying the deSolve package [19].

Results

Data

Median plasma concentration–time profiles demonstrated plasma accumulation after multiple dose inhalations both in healthy volunteers and patients. For both these groups, a high terminal half-life can be observed, causing low variability (peak-to-trough) in plasma concentrations up to 24 h. In comparison to healthy volunteers, both asthma and COPD patients demonstrate slightly increased maximum plasma concentrations and slightly higher trough plasma concentrations at 24 h after multiple dose inhalations (see Figure 1).

Model development

By applying a population PK approach, it was demonstrated that the PK data after olodaterol inhalation (healthy, asthma, COPD) was best described by three parallel pulmonary absorption processes: fast, intermediate and slow (see Figure 2). The PBIO was estimated to be 48.7% (46.1–51.3%, 95% CI) of the nominal dose in patients with asthma and 53.6% (51.1–56.2%) in patients with COPD. In asthmatic patients 87.2% (85.4–88.8%) of the PBIO was slowly absorbed with an absorption half-life of 18.5 h (16.3–21.4 h), whereas in COPD patients 80.1% (78.0–82.2%) of the PBIO was slowly absorbed

Table 2

Investigated covariate-parameter relations including a short description of the (physiological) rationale

PK parameter	Covariate	(Physiological) rationale + reference*
Pulmonary bioavailable fraction	Disease status (healthy, asthma, COPD)	<ul style="list-style-type: none"> • Narrowed airways in asthmatic and COPD patients [9] • Different inhalation patterns [9] • Different pulmonary bioavailable fractions/exposures demonstrated for, for example, fluticasone propionate [11]
	BSA	<ul style="list-style-type: none"> • Increased airway and lung volumes and different inhalation in healthy volunteers with higher BSA [36]
	Age	<ul style="list-style-type: none"> • Reduced rates of pulmonary ventilation in elderly patients [37]
	Smoking status (non-smoker, ex-smoker, smoker)	<ul style="list-style-type: none"> • Enhanced airway responsiveness in smoker [38]
	Ethnicity (Caucasian, Asian, Black)	<ul style="list-style-type: none"> • Increased exposure after indacaterol inhalation in Asians [39, 40]
	Sex (male, female)	<ul style="list-style-type: none"> • Different lung volumes, increased pulmonary deposition in females [41]
Proportionality factors (characterizing the proportions absorbed by a specific absorption process)	Disease status (healthy, asthma, COPD)	<ul style="list-style-type: none"> • Narrowed airways in asthmatic and COPD patients [9] • Mucus plugging in patients [9] • Different deposition patterns (more central in patients) [9]
	BSA	<ul style="list-style-type: none"> • Increased airway and lung volumes in healthy volunteers with higher BSA and different inhalation patterns [36]
	Age	<ul style="list-style-type: none"> • Reduced rates of ventilation in elderly patients [37]
	Smoking status (non-smoker, ex-smoker, smoker)	<ul style="list-style-type: none"> • Enhanced airway responsiveness in smokers [38]
	Ethnicity (Caucasian, Asian, Black)	<ul style="list-style-type: none"> • Smaller lungs and smaller airways in Asians were discussed to influence fluticasone furoate PK after inhalation [42]
	Sex (male, female)	<ul style="list-style-type: none"> • Differences in regional pulmonary deposition patterns [41]
Absorption rate constants	Disease status (healthy, asthma, COPD)	<ul style="list-style-type: none"> • Airway remodelling in patients [43, 44] • Higher vascularization in patients [45]
	Age	<ul style="list-style-type: none"> • Thickened airway epithelia in elderly [37]
	Smoking status (non-smoker, ex-smoker, smoker)	<ul style="list-style-type: none"> • Tight junctions inhibited in smokers [46] • Faster pulmonary absorption demonstrated for inhaled insulin in smokers [47]

*The provided references present selected examples as rationale for investigating specific covariates on the PK parameters. Provided covariates were only investigated to have an effect on PK parameters with between-subject variability associated, for example, if an absorption rate constant was not characterized with variability in the base model, the listed covariates were not investigated on the specific absorption rate constant. BSA: body surface area; PK: pharmacokinetic.

with an absorption half-life of 37.8 h (31.1–47.8 h). In comparison, healthy volunteers had a PBIO of 48.7% (46.1–51.3%) and a proportion of 74.6% (69.1–80.2%) was estimated to be slowly absorbed with an absorption half-life of 18.5 h (16.3–21.4 h). These re-estimated healthy volunteer PK parameters in this analysis of combined data were in agreement with healthy volunteer PK parameters estimated based only on PK data from healthy volunteers: previous bioavailable fraction: 49.4%, previous proportion slowly absorbed: 70.1% [6]. All final parameter estimates including the relative standard errors are given in Table 3.

By applying a FFEM approach including model reduction, four covariates were identified with statistically significant influence on one or more of the four pulmonary PK parameters (associated with BSV, see below): disease status, ethnicity, smoking status and BSA (see also Figure 2, covariates displayed in black boxes). The decrease in the OFV by including the 11 covariate-parameter relations compared to the

base model was substantial (approximately 215 points). The underlying disease had a stronger impact on the absorption characteristics (absorption rate constant, proportions absorbed), other covariates had more pronounced impact on the PBIO; e.g., it was estimated that healthy Asians had a PBIO of 71.8%. A full list of the covariate parameter estimates (and the relative standard errors) is given in Table 3. Some covariate-parameter relations were quantified on the logit scale and might be difficult to interpret based on the covariate estimates alone. Hence, the resulting absorption characteristics separated by covariate can be found in Table 4. Other investigated covariates effects, not listed in Table 4, were not found to be statistically significant and only had a minor influence on estimated PK parameters (e.g., sex or age) and were removed during the model reduction process.

Remaining (unexplained) BSV after covariate inclusion was identified for four pulmonary PK parameters; (1) the PBIO (25.2% coefficient of variation (CV)), (2) the

Table 3

Estimated parameters for the developed model describing the PK after inhalation in healthy volunteers, patients with asthma, and patients with COPD

Parameter	Abbreviation	Unit	Population estimate (%RSE)	BSV, %CV (%RSE)
Systemic disposition model [6]				
Central volume of distribution (CMT 1)*	V_C	[l]	23.5 (4.35)	26.2 (10.4)
Peripheral volume of distribution (CMT 2)*	V_2	[l]	2590 (35.7)	—
Peripheral volume of distribution (CMT 3)*	V_3	[l]	473 (10.7)	—
Peripheral volume of distribution (CMT 4)*	V_4	[l]	16.1 (19.7)	—
Inter-compartmental clearance (to CMT 2)*	Q_2	[l h ⁻¹]	31.7 (12.3)	25.7 (13.5)
Inter-compartmental clearance (to CMT 3)*	Q_3	[l h ⁻¹]	65.7 (5.28)	16.8 (13.5)
Inter-compartmental clearance (to CMT 4)*	Q_4	[l h ⁻¹]	22.5 (8.06)	—
Renal clearance *	CL_R	[l h ⁻¹]	10.5 (4.55)	—
Non-renal clearance *	CL_{NR}	[l h ⁻¹]	63.7 (8.49)	26.8 (13.5)
Pulmonary absorption model (reference healthy volunteer, non-smoker, Caucasian, BSA: 1.89 m²)				
Slow absorption rate constant	$k_{a(slow)}$	[h ⁻¹]	0.0375 (6.91)	88.5 (4.85)
Intermediate absorption rate constant	$k_{a(int)}$	[h ⁻¹]	0.447 (3.65)	—
Fast absorption rate constant	$k_{a(fast)}$	[h ⁻¹]	2.41 (12.1)	62.6 (6.09)
Pulmonary bioavailable Fraction	PBIO	[% ND]	48.7 (2.71)	BSV: 25.2 (7.88) BOV: 37.0 (2.60)
First proportionality factor	PF1	—	0.746 (3.79)	20.1 (4.76)
Second proportionality factor	PF2	—	0.850 (0.691)	—
Fraction slowly absorbed [†]	—	[% PBIO]	74.6 [‡]	—
Fraction intermediately absorbed [†]	—	[% PBIO]	21.6 [§]	—
Fraction fast absorbed [†]	—	[% PBIO]	3.81 [¶]	—
Covariate model*				
COPD on the PBIO	—	—	0.198 (36.3)	—
COPD on PF1	—	—	0.312 (51.9)	—
COPD on $k_{a(slow)}$	—	—	-0.509 (11.2)	—
COPD on $k_{a(fast)}$	—	—	0.808 (27.4)	—
Asthma on PF1	—	—	0.834 (19.8)	—
Asthma on $k_{a(fast)}$	—	—	0.928 (28.2)	—
Smoking on $k_{a(slow)}$	—	—	-0.235 (38.9)	—
Smoking on $k_{a(fast)}$	—	—	0.562 (26.7)	—
BSA on the PBIO	—	[m ⁻²]	-0.815 (19.0)	—
Black on the PBIO	—	—	0.358 (36.8)	—
Asian on the PBIO	—	—	0.989 (38.0)	—
Residual variability model				
Proportional residual variability (plasma)	—	[% CV]	23.3 (0.562)	—
Proportional residual variability (urine)	—	[% CV]	48.8 (0.909)	—

*Covariates are represented in the form of the parameter estimates, which are implemented as described in the methods section. Transformed pulmonary absorption characteristics for every covariate can be found in Table 4. †Transformed parameters derived from the model estimates. ‡Value equal to PF1. §Calculated by $(1 - PF1) * PF2$. ¶Calculated by $(1 - PF1) * (1 - PF2)$, also see methods section. BSV: between-subject variability; BOV: between-occasion variability; CV: coefficient of variation; ND: nominal dose (ex-mouthpiece); PBIO: pulmonary bioavailable fraction; RSE: relative standard error.

Table 4

Pulmonary absorption characteristics dependent on subject-specific factors (covariates) including the 95% confidence intervals*

Scenarios [†]	Pulmonary bioavailable fraction (PBIO) [% of nominal dose]		Slow absorption process		Intermediate absorption process		Fast absorption process	
			Fraction of PBIO [%]	Absorption half-life [h]	Fraction of PBIO [%]	Absorption half-life [h]	Fraction of PBIO [%]	Absorption half-life [min]
"Standard" healthy volunteer (BSA: 1.89 m², non-smoker, Caucasian)	48.7 (46.1–51.3)		74.6 (69.1–80.2)	18.5 (16.3–21.4)	21.6 (16.8–26.3)	1.55 (1.45–1.67)	3.81 (2.95–4.70)	17.3 (14.0–22.6)
Patient with asthma (BSA: 1.89 m², non-smoker, Caucasian)	48.7 (46.1–51.3)		87.2 (85.4–88.8)	18.5 (16.3–21.4)	10.9 (9.50–12.4)	1.55 (1.45–1.67)	1.92 (1.66–2.22)	9.08 (7.76–10.9)
Patient with COPD (BSA: 1.89 m², non-smoker, Caucasian)	53.6 (51.1–56.2)		80.1 (78.0–82.2)	37.8 (31.1–47.8)	16.9 (15.1–18.8)	1.55 (1.45–1.67)	2.98 (2.64–3.35)	9.70 (8.30–11.5)
Black healthy volunteer (BSA: 1.89 m², non-smoker, Black)	57.6 (51.0–63.9)		74.6 (69.1–80.2)	18.5 (16.3–21.4)	21.6 (16.8–26.3)	1.55 (1.45–1.67)	3.81 (2.95–4.69)	17.3 (14.0–22.6)
Asian healthy volunteer (BSA: 1.89 m², non-smoker, Asian)	71.8 (55.2–84.1)		74.6 (69.1–80.2)	18.5 (16.3–21.4)	21.6 (16.8–26.3)	1.55 (1.45–1.67)	3.81 (2.96–4.70)	17.3 (14.0–22.6)
Smoking healthy volunteer (BSA: 1.89 m², smoker, Caucasian)	48.7 (46.1–51.3)		74.6 (69.1–80.2)	24.3 (19.3–31.9)	21.6 (16.8–26.3)	1.55 (1.45–1.67)	3.81 (2.95–4.69)	11.2 (8.79–14.7)
Light healthy volunteer (BSA: 1.49 m², non-smoker, Caucasian)	56.8 (52.8–60.7)		74.6 (69.1–80.1)	18.5 (16.3–21.4)	21.6 (16.9–26.3)	1.55 (1.45–1.67)	3.81 (2.96–4.70)	17.3 (14.0–22.6)
Heavy healthy volunteer (BSA: 2.29 m², non-smoker, Caucasian)	40.7 (36.9–44.5)		74.6 (69.0–80.2)	18.5 (16.3–21.4)	21.6 (16.8–26.3)	1.55 (1.45–1.67)	3.81 (2.95–4.70)	17.3 (14.0–22.6)
Highest lung disposition scenario (COPD, BSA: 1.49 m², smoker, Asian)	81.1 (67.1–90.1)		80.1 (78.0–82.2)	49.8 (40.6–62.8)	16.9 (15.1–18.8)	1.55 (1.45–1.67)	2.98 (2.63–3.35)	6.22 (5.29–7.46)

*Different absorption characteristics compared to the "standard healthy volunteer" are indicated in bold and underlined. †Population characteristics do not necessarily reflect realistic population-specific factors, e.g., Asians usually have lower BSA compared to Caucasians. However, to perform univariate comparisons, this simplification is performed. Absorption half-lives are calculated by $\ln(2)/k_a$. BSA: body surface area; PBIO: pulmonary bioavailable fraction.

proportionality factor quantifying the slowly absorbed proportion (20.1% CV), (3) the fast (62.6% CV), and (4) the slow absorption rate constant (88.5% CV). BOV was identified for the PBIO (37.0% CV).

VPCs stratified for disease status (healthy, asthma, COPD) are shown in Figure S1, and standard GOF plots for plasma in Figure S2 and for urine in Figure S3 of the online supplementary material. Both VPCs and GOF plots demonstrated overall good model performance. The VPCs indicated that the median time profiles and the 2.5th percentiles of the observed data were well predicted. The 97.5th percentiles of both plasma concentration and urine concentration–time profiles were underpredicted in COPD patients. The good prediction of both the median and lower percentile, but underprediction of the upper percentile indicates that the variability especially in COPD patients is not well captured. However, additional (between-subject) variability terms could not be adequately estimated based on the available data. In addition, GOF plots indicated some outliers with high conditional weighted or individual weighted residuals (CWRES and IWRES). The NONMEM code of the developed pulmonary PK model is provided in the online supplementary material.

Model-based simulations

A summary of the magnitude of all covariate influences on C_{max} , AUC_{Plasma} and AUC_{Lung} both after single dose and at steady state, including model imprecision, is provided in Table 5, and PK metrics at steady state including the 95% CI are additionally visualized in Figure 3. C_{max} was lower in patients compared to healthy volunteers; 32% lower after single dose and 20% lower at steady state in patients with asthma, and 24% lower and 8.5% lower for patients with COPD, respectively. This was in disagreement with the observed median plasma concentration–time profiles (Figure 1). Higher observed C_{max} in asthmatic and COPD patients can instead be attributed to different subject-specific factors compared to healthy volunteers; smoking, lower BSA, as well as Asian or Black ethnicity increased the C_{max} both after single dose and at steady state. As can be seen in Figure 3, Asian and Black ethnicity also increased the $AUC_{Plasma,SS}$ by 41% and 27%, respectively compared to healthy Caucasians. A lower BSA (1.49 m² relative to 1.89 m²) increased the $AUC_{Plasma,SS}$ by 17%, while a higher BSA (2.29 m²) conversely decreased the $AUC_{Plasma,SS}$ by 17%. Compared to the standard healthy volunteer, the $AUC_{Lung,SS}$ was 13% higher in patients with asthma and even 143% higher in patients with COPD. Overall precision of the simulated PK metrics was characterized by CVs of less than 10%.

A comparison of individual $C_{max,SS}$, $AUC_{Plasma,SS}$ and $AUC_{Lung,SS}$ distributions (including BSV and BOV) between patients and healthy volunteers with different subject-specific factors is provided in Figure 4. Results after single dose and the corresponding 95% confidence intervals of all PK metrics are given in the online supplementary material. The 95% confidence intervals for the $C_{max,SS}$, $AUC_{Plasma,SS}$ and $AUC_{Lung,SS}$ in healthy volunteers ranged from 1.1 to 7.4 pg ml⁻¹, from 13 to 59 pg h ml⁻¹ and from 7.6 to 196 pg h, respectively. The respective intervals for the “highest lung disposition” scenario (COPD, BSA 1.49 m², smoker, Asian)

ranged from 1.9 to 9.6 pg ml⁻¹, from 26 to 74 pg h ml⁻¹ and from 45–640 pg h. The highest numerical difference between the standard healthy volunteer and the “highest lung disposition” scenario was an increase in $AUC_{Lung,SS}$ by 366% (calculated based on the median), followed by a 57% increase in $AUC_{Plasma,SS}$ and a 56% increase in $C_{max,SS}$. These results indicate that a change in pulmonary PK after drug inhalation in patient populations can translate into smaller changes in systemic PK.

Discussion

Based on a population PK approach and a large amount of PK data, the systemic and pulmonary PK of olodaterol in patients with asthma or COPD were successfully quantified and compared to each other as well as to healthy volunteers. The PBIO after oral olodaterol inhalation with the Respimat® device was comparable between all three populations of interest (asthma, COPD, healthy volunteers). Only a 10% relative difference was demonstrated between healthy volunteers and COPD patients. There was no significant difference in the PBIO between healthy volunteers and asthmatic patients. In comparison, the bioavailability after nedocromil inhalation with a pressurized metered dose inhaler (pMDI) was reduced by approximately 40% in patients with asthma compared to healthy volunteers [20] and after inhalation of fluticasone propionate with a pMDI the difference was even more pronounced with more than 50% lower bioavailability in patients with asthma [10]. A higher centrally deposited fraction of particles in patients compared to healthy volunteers [8, 21] combined with a faster mucociliary clearance of non-dissolved particles in the central conducting airways compared to the peripheral airways [21–23] was discussed as an explanation for the reduced bioavailability of fluticasone propionate. In contrast to fluticasone propionate, olodaterol is inhaled in the form of a solution and therefore the influence of the mucociliary clearance on the (pulmonary) bioavailability is expected to be negligible. Based on a comparable PBIO between healthy volunteers, patients with asthma and patients with COPD, it can be concluded for olodaterol inhaled with the Respimat® that a comparable fraction of the nominal dose is being absorbed to lung tissue, which represents the effect site for inhaled β_2 -sympathomimetic drugs [24, 25].

Overall, slow absorption kinetics were demonstrated for patients with asthma and patients with COPD, and only a small proportion was fast absorbed. In patients with COPD, 80.1% of PBIO was absorbed with an absorption half-life of approximately 38 h, which was roughly twice the absorption half-life of 18.5 h estimated for healthy volunteers and asthmatic patients. In patients with asthma, a higher proportion of 87.5% was slowly absorbed; the slow absorption half-life was in agreement with the estimate in healthy volunteers (no significant difference). As a consequence of the different absorption half-lives and despite comparable PBIO, the simulated $AUC_{Lung,SS}$ were approximately 13% and 143% higher in asthmatic and COPD patients at steady state compared to healthy volunteers, respectively.

Table 5

Influence of covariate effects on C_{max} , AUC_{Plasma} and AUC_{Lung} accounting for model imprecision after single dose (0 - 24 h) and at steady state (assumed after 14 once-daily inhaled doses of 5 µg) of orally inhaled olodaterol including the 95% confidence interval ($n = 1000$ simulations per scenario)

Scenarios*	C_{max} [$\mu\text{g ml}^{-1}$]		AUC_{Plasma} [$\mu\text{g h ml}^{-1}$]		AUC_{Lung} [$\mu\text{g h}$]	
	Single dose	Steady state	Single dose	Steady state	Single dose	Steady state
“Standard” healthy volunteer (BSA: 1.89 m ² , non-smoker, Caucasian)	2.03 (1.65–2.41)	2.94 (2.58–3.31)	14.7 (13.5–15.9)	32.1 (30.3–33.7)	29.9 (27.0–33.0)	49.7 (42.4–57.9)
Patient with Asthma (BSA: 1.89 m ² , non-smoker, Caucasian)	1.38 (1.15–1.62)	2.35 (2.12–2.59)	13.5 (12.4–14.6)	32.0 (30.4–33.6)	33.5 (31.0–36.4)	56.1 (48.4–66.1)
Patient with COPD (BSA: 1.89 m ² , non-smoker, Caucasian)	1.54 (1.24–1.89)	2.70 (2.41–3.05)	10.5 (9.44–11.5)	34.6 (32.9–36.2)	44.1 (40.9–47.0)	121 (105–142)
Black healthy volunteer (BSA: 1.89 m ² , non-smoker, Black)	2.58 (2.09–3.03)	3.74 (3.28–4.16)	18.6 (17.2–20.0)	40.7 (39.3–42.3)	38.0 (34.8–41.5)	63.4 (54.7–73.9)
Asian healthy volunteer (BSA: 1.89 m ² , non-smoker, Asian)	2.86 (2.37–3.38)	4.15 (3.71–4.63)	20.7 (19.1–22.2)	45.3 (43.9–46.6)	42.4 (38.7–46.6)	70.7 (60.4–84.1)
Smoking healthy volunteer (BSA: 1.89 m ² , smoker, Caucasian)	2.13 (1.73–2.55)	3.07 (2.69–3.46)	13.4 (12.2–14.6)	31.9 (30.2–33.5)	32.0 (29.2–35.4)	61.0 (51.8–72.9)
Light healthy volunteer (BSA: 1.49 m ² , non-smoker, Caucasian)	2.35 (1.94–2.84)	3.41 (2.99–3.91)	17.1 (15.6–18.8)	37.4 (34.7–39.8)	35.0 (31.4–38.9)	57.9 (49.2–69.5)
Heavy healthy volunteer (BSA: 2.29 m ² , non-smoker, Caucasian)	1.69 (1.40–2.01)	2.44 (2.15–2.79)	12.2 (10.9–13.6)	26.8 (24.3–29.5)	25.0 (21.9–28.6)	41.4 (34.6–50.3)
Highest lung disposition scenario (COPD, BSA: 1.49 m², smoker, Asian)	3.14 (2.53–3.83)	4.76 (4.18–5.43)	15.7 (14.1–17.4)	49.9 (47.9–51.6)	61.2 (56.6–65.7)	188 (163–220)

*To allow for comparison of the univariate evaluation of the covariate effects, population characteristics of some scenarios might not necessarily reflect realistic population-specific factors, e.g., Asians usually have lower BSA compared to Caucasians. AUC_{Lung} : area of unabsorbed amount under the curve; AUC_{Plasma} : area of the plasma concentration under the curve; BSA: body surface area; C_{max} : maximum plasma concentration; COPD: chronic obstructive pulmonary disease.

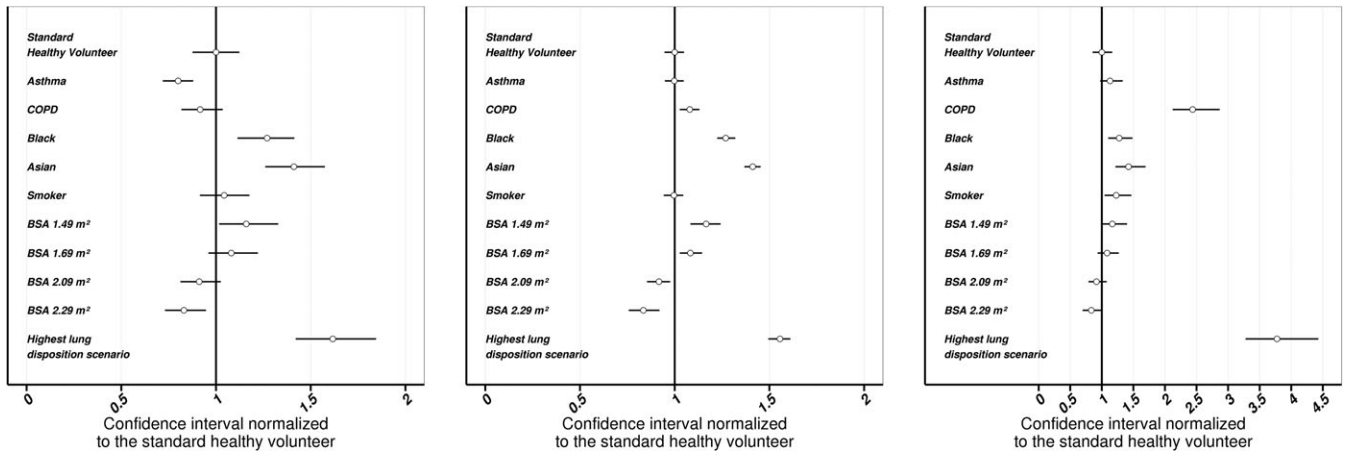


Figure 3

PK metrics at steady state (left: C_{max} , middle: AUC_{Plasma} , right: AUC_{Lung}), including overall model imprecision after oral olodaterol inhalation. Presented metrics are normalized to the median PK metric of standard healthy volunteer (BSA: 1.89 m², non-smoker, Caucasian). Points: normalized median PK metrics, lines: normalized 95% confidence intervals. AUC_{Plasma} : area under the plasma concentration–time profile at steady-state (0–24 h after inhalation, $n = 14$ doses), AUC_{Lung} : Area under the unabsorbed amount–time profile at steady-state (0–24 h after inhalation, $n = 14$), BSA: body surface area, “highest lung disposition scenario”: COPD, BSA 1.49 m², smoker, and Asian

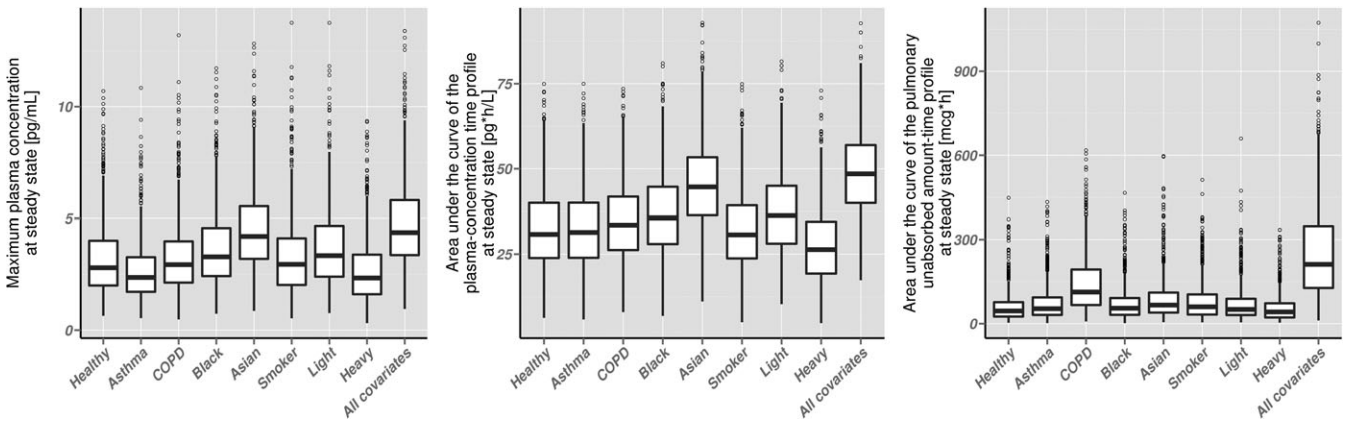


Figure 4

Box-and-whisker plots of simulation-based pharmacokinetic metrics at steady state (14 once-daily inhaled doses of 5 µg, $n = 1000$ for each covariate). Simulations were performed with the developed PK model and accounted for between-subject and between-occasion variability. Left plot: maximum plasma concentration; middle plot: area under the curve of the plasma concentration–time profile; right plot: area under the curve of the unabsorbed drug amount–time profile; thick black line: median; lower and top border of the boxes: 25th percentile and 75th percentile; lower and upper end of the whisker: lowest and highest value within the range of the median ± 1.5 times the interquartile range; points: PK metrics outside the whisker range

Differences in the pulmonary PK between patients and healthy volunteers might be explained based on different airway characteristics between patients and healthy volunteers (see Table 2), such as inflammatory processes in patients that can cause damage to the epithelial airway barriers [26]. Differing proportions absorbed (e.g., higher proportion slowly absorbed in asthmatic patients) might be the result of differing pulmonary deposition patterns in patients and healthy volunteers [8]. However, even for healthy volunteers it was not possible to quantitatively associate the different pulmonary absorbed proportions of inhaled olodaterol to pulmonary deposition patterns [6]. Thus, for patients this

association might be even more challenging. However, qualitatively a higher slowly absorbed proportion of olodaterol in patients is in agreement with a more central pulmonary deposition pattern in patients compared to healthy volunteers [8].

When comparing different subpopulations, as in this case patients and healthy volunteers, it is also important to consider demographical differences; asthmatic patients had a lower BSA and were older (see Table 1). In contrast to healthy volunteers, COPD patients comprised a higher fraction of smokers, were older and therefore had potentially a lower creatinine clearance (based on the Cockcroft-Gault equation

[27]). The range of patient demographic values was higher in patients compared to healthy volunteers. In addition, healthy volunteers comprised only Caucasians, whereas Asian and Black asthmatic and COPD patients were included in the dataset. Based on these demographical differences, differences in PK between asthma, COPD and healthy volunteers, such as a higher C_{max} or a higher exposure in patients can also be attributed to other covariate effects such as smoking or differing BSA.

In contrast to healthy volunteers, no IV PK data in asthmatic or COPD patients were available for development of the systemic PK disposition model. Therefore, the systemic disposition was assumed to be comparable between patients and healthy volunteers. Applying the same systemic PK disposition model appeared to be a reasonable assumption based on the following considerations: (1) neither IV nor inhalation PK data indicated an influence of age or creatinine clearance on any systemic or pulmonary disposition parameter; (2) renal elimination accounted for only 14.2% of olodaterol clearance based on modelling results [6]; and (3) it was demonstrated that a decrease in renal or hepatic function has only a small influence on the systemic PK of olodaterol [28]. However, covariate–parameter relations that could not be adequately investigated based on IV PK data might be misinterpreted; for example, the influence of ethnicity on pulmonary PK parameters might be an artefact due to an unknown confounding covariate–parameter relationship in the systemic disposition model.

Performing simulations accounting for BSV and BOV demonstrated that covariate effects on pulmonary PK parameters impact C_{max} , AUC_{Plasma} and AUC_{Lung} (see Figure 4). In comparison to the overall variability which can be attributed to (unexplained) BSV and BOV, the explained variability by covariate–PK parameter relations was lower (see Figure 4). The finding that BOV is higher in BSV was in agreement with results from Borgström et al. who demonstrated a higher lung deposition variability within patients compared to between patients (for a dry powder inhaler) [4]. Unexplained between-subject (pulmonary) PK variability can depend, e.g., on individual mouth-throat geometries [29], individual airway diameters [30], or other individual airway characteristics. BOV can depend, e.g., on the inhalation patterns [31] or the patient performance in handling the device, which can vary for each drug inhalation [4]. However, individual mouth-throat/airway geometries and inhalation patterns were not available. Thus, the influence of these characteristics on the pulmonary and systemic PK remains to be quantified.

Given remaining overall (pulmonary) PK variability, even the statistically significant covariate–parameter relations have to be evaluated in this context. The influence of covariates on the pulmonary fate was of a larger magnitude compared to the influence on systemic exposure, indicating comparable systemic safety profiles in patients and healthy volunteers. Furthermore, this results in a 13.1% and 126% higher ratio of $AUC_{Lung,SS}$ to $AUC_{Plasma,SS}$ in patients with asthma and COPD, respectively, compared to healthy volunteers (comparison between unabsorbed amount and concentrations). These higher lung-to-systemic ratios indicate a more beneficial pulmonary targeting in patients in general and especially in COPD. Based on the performed

PK investigations, the typical healthy volunteer would have the lowest therapeutic ratio, whereas all significant covariates either increase the therapeutic ratio or can be considered neutral. Thus, based on the $AUC_{Lung,SS}$ to $AUC_{Plasma,SS}$ ratios, a healthy volunteer can be considered as a worst case scenario. However, directly linking pulmonary unabsorbed drug amounts to pulmonary PD might represent a marked simplification, because the drug amount unabsorbed does not necessarily represent free drug concentrations, which might be more relevant for pulmonary efficacy. The relationship between unabsorbed amount and free pulmonary olodaterol concentrations or pulmonary β_2 -receptor occupancy therefore remains to be further investigated, e.g. by *in vitro* assays [32].

The demonstrated long pulmonary residence time for olodaterol was previously proposed for another long-acting inhaled β_2 -sympathomimetic drug (AZD3199) to result in a higher therapeutic index compared to formoterol [33]. In comparison to olodaterol with a log D of 1.2 at pH 7.4 [7], AZD3199 represents a more lipophilic drug with a log P of 6.0 [34] and is even more lipophilic than inhaled corticosteroids (fluticasone propionate has a log P of 3.89 [35]). Due to slow dissolution kinetics for lipophilic inhaled corticosteroids, the fraction of drug cleared from the lungs by the mucociliary clearance was proposed to be high, especially in patients (see above). However, this can be excluded for olodaterol as it is inhaled in the form of a solution and the pulmonary bioavailable fractions were comparable for patients and healthy volunteers. Consequently, the demonstrated long pulmonary retention of olodaterol was not dissolution-related, potentially causing the low influence of the pulmonary disease on the drug amount being absorbed to the target lung tissue. This might provide a substantial benefit over slowly dissolving dry powder formulations. In conclusion, previous proposals that the long pulmonary retention of inhaled olodaterol might contribute to its long-lasting efficacy can be considered as representative for patients with pulmonary diseases.

Conclusion

By applying a population PK approach, it was demonstrated for olodaterol administered with the Respimat® that asthma and COPD only had a minor influence on the PBIO, with values ranging from 48.7% for healthy volunteers and patients with asthma to 53.6% for patients with COPD. Long pulmonary residence times were demonstrated for a large proportion of the PBIO both in patients with asthma (87.2% with $t_{1/2}$ of 18.5 h) and with COPD (80.1% with $t_{1/2}$ of 37.8 h). This long pulmonary residence time can be considered beneficial for efficient lung targeting and a long drug efficacy in patients.

Competing Interests

All authors have completed the Unified Competing Interest form at http://www.icmje.org/coi_disclosure.pdf (available on request from the corresponding author) and declare that

Benjamin Weber, Alexander Staab and Christina Kunz are employees of Boehringer Ingelheim Pharma GmbH & Co. KG. The PhD project of Jens Markus Borghardt is funded by Boehringer Ingelheim GmbH & Co. KG. Charlotte Kloft reports grants from an industry consortium (AbbVie Deutschland GmbH & Co. KG, Boehringer Ingelheim Pharma GmbH & Co. KG, F. Hoffmann-La Roche Ltd, Merck KGaA, and SANOFI) and grants from Innovative Medicines Initiative-Joint Undertaking (“DDMoRe”), both outside the submitted work. The authors declare no further conflicts of interest.

References

- Global Initiative for Chronic Obstructive Lung Disease (GOLD). Global Strategy for the Diagnosis, Management, and Prevention of Chronic Obstructive Pulmonary Disease, 2015. Available at http://www.goldcopd.it/materiale/2015/GOLD_Report_2015.pdf
- Global Initiative for Asthma (GINA). Global strategy for asthma management and prevention, 2016. <http://ginasthma.org/2016-gina-report-global-strategy-for-asthma-management-and-prevention/>
- Borgström L, Derom E, Ståhl E, Wåhlin-Boll E, Pauwels R. The inhalation device influences lung deposition and bronchodilating effect of terbutaline. *Am J Respir Crit Care Med* 1996; 153: 1636–40.
- Borgström L, Bengtsson T, Derom E, Pauwels R. Variability in lung deposition of inhaled drug, within and between asthmatic patients, with a pMDI and a dry powder inhaler, Turbuhaler®. *Int J Pharm* 2000; 193: 227–30.
- Parra-Guillen Z, Weber B, Sharma A, Freijer J, Retlich S, Borghardt JM, *et al.* Population pharmacokinetic analysis of tiotropium in healthy volunteers after intravenous administration and inhalation. *J Pharmacokinet Pharmacodyn* 2014; 41: S54.
- Borghardt JM, Weber B, Staab A, Kunz C, Formella S, Kloft C. Investigating pulmonary and systemic pharmacokinetics of inhaled olodaterol in healthy volunteers using a population pharmacokinetic approach. *Br J Clin Pharmacol* 2016; 81: 538–52.
- Casarosa P, Kollak I, Kiechle T, Ostermann A, Schnapp A, Kiesling R, *et al.* Functional and biochemical rationales for the 24-hour-long duration of action of olodaterol. *J Pharmacol Exp Ther* 2011; 337: 600–9.
- Darquenne C. Aerosol deposition in health and disease. *J Aerosol Med Pulm Drug Deliv* 2012; 25: 140–7.
- Barnes PJ, Drazen J, Rennard SI, Thomson NC, eds. *Asthma and COPD: Basic Mechanisms and Clinical Management*, 2nd edn. Amsterdam: Elsevier, 2009.
- Brutsche MH, Brutsche IC, Munavvar M, Langley SJ, Masterson CM, Daley-Yates P, *et al.* Comparison of pharmacokinetic and systemic effects of inhaled fluticasone propionate in patients with asthma and healthy volunteers: a randomised crossover study. *Lancet* 2000; 356: 556–61.
- Hallett C. Corticosteroid treatment of asthma: now at the crossroads. *Respir Med* 1999; 93: 292–4.
- Bartels C, Looby M, Sechaud R, Kaiser G. Determination of the pharmacokinetics of glycopyrronium in the lung using a population pharmacokinetic modelling approach. *Br J Clin Pharmacol* 2013; 76: 868–79.
- Dershwitz M, Walsh JL, Morishige RJ, Connors PM, Rubsamen RM, Shafer SL, *et al.* Pharmacokinetics and pharmacodynamics of inhaled versus intravenous morphine in healthy volunteers. *Anesthesiology* 2000; 93: 619–28.
- Krishnaswami S, Hochhaus G, Möllmann H, Barth J, Derendorf H. Interpretation of absorption rate data for inhaled fluticasone propionate obtained in compartmental pharmacokinetic modeling. *Int J Clin Pharmacol Ther* 2005; 43: 117–22.
- Bonate PL. *Pharmacokinetic-Pharmacodynamic Modeling and Simulation*, 2nd edn. New York: Springer Science and Business Media, 2011.
- Gastonguay MR. Full Covariate Models as an Alternative to Methods Relying on Statistical Significance for Inferences about Covariate Effects: A Review of Methodology and 42 Case Studies. PAGE. Abstracts of the Annual Meeting of the Population Approach Group in Europe, Abstr 2229, Athen, Greece.
- Keizer RJ, Karlsson MO, Hooker A. Modeling and simulation workbench for NONMEM: Tutorial on Pirana, PsN, and Xpose. *CPT Pharmacometrics Syst Pharmacol* 2013; 2: e50
- R Core Team. R: A Language and Environment for Statistical Computing. Vienna: R Foundation for Statistical Computing, 2014.
- Soetaert K, Petzoldt T, Setzer RW. Solving differential equations in R: Package deSolve. *J Stat Software* 2010; 33: 1–25.
- Neale MG, Brown K, Foulds RA, Lal S, Morris DA, Thomas D. The pharmacokinetics of nedocromil sodium, a new drug for the treatment of reversible obstructive airways disease, in human volunteers and patients with reversible obstructive airways disease. *Br J Clin Pharmacol* 1987; 24: 493–501.
- Edsbacker S, Wollmer P, Selroos O, Borgstrom L, Olsson B, Ingelf J. Do airway clearance mechanisms influence the local and systemic effects of inhaled corticosteroids? *Pulm Pharmacol Ther* 2008; 21: 247–58.
- Smaldone GC, Perry RJ, Bennett WD, Messina MS, Zwang J, Ilowite J. Interpretation of “24 hour lung retention” in studies of mucociliary clearance. *J Aerosol Med* 1988; 1: 11–20.
- Foster WM, Langenback E, Bergofsky EH. Measurement of tracheal and bronchial mucus velocities in man: relation to lung clearance. *J Appl Physiol Respir Environ Exerc Physiol* 1980; 48: 965–71.
- Usmani OS, Barnes PJ. Assessing and treating small airways disease in asthma and chronic obstructive pulmonary disease. *Ann Med* 2012; 44: 146–56.
- Usmani OS, Biddiscombe MF, Barnes PJ. Regional lung deposition and bronchodilator response as a function of β_2 -agonist particle size. *Am J Respir Crit Care Med* 2005; 172: 1497–504.
- Aoshiba K, Nagai A. Differences in airway remodeling between asthma and chronic obstructive pulmonary disease. *Clin Rev Allergy Immunol* 2004; 27: 35–43.
- Cockcroft DW, Gault MH. Prediction of creatinine clearance from serum creatinine. *Nephron* 1976; 16: 31–41.
- Kunz C, Luedtke D, Unseld A, Hamilton A, Halabi A, Wein M, *et al.* Pharmacokinetics and safety of olodaterol administered with the Respimat Soft Mist inhaler in subjects with impaired hepatic or renal function. *Int J Chron Obstruct Pulmon Dis* 2016; 11: 585–95.
- Grgic B, Finlay WH, Burnell PKP, Heenan AF. *In vitro* intersubject and intrasubject deposition measurements in realistic mouth-throat geometries. *Aerosol Sci* 2004; 35: 1025–40.

- 30 Asgharian B, Price OT, Hofmann W. Prediction of particle deposition in the human lung using realistic models of lung ventilation. *Aerosol Sci* 2006; 37: 1209–21.
- 31 Brand P, Hederer B, Austen G, Dewberry H, Meyer T. Higher lung deposition with Respimat® Soft Mist™ inhaler than HFA-MDI in COPD patients with poor technique. *Int J COPD* 2008; 3: 763–70.
- 32 Bäckström E, Lundqvist A, Boger E, Svanberg P, Ewing P, Hammarlund-Udenaes M, *et al.* Development of a novel lung slice methodology for profiling of inhaled compounds. *J Pharm Sci* 2016; 105: 838–45.
- 33 Bjermer L, Rosenborg J, Bengtsson T, Lotvall J. Comparison of the bronchodilator and systemic effects of AZD3199, an inhaled ultra-long-acting beta(2)-adrenoceptor agonist, with formoterol in patients with asthma. *Ther Adv Respir Dis* 2013; 7: 264–71.
- 34 Stocks MJ, Alcaraz L, Bailey A, Bonnert R, Cadogan E, Christie J, *et al.* Discovery of AZD3199, an inhaled ultralong acting beta2 receptor agonist with rapid onset of action. *ACS Med Chem Lett* 2014; 5: 416–21.
- 35 Daley-Yates PT. Inhaled corticosteroids: potency, dose equivalence and therapeutic index. *Br J Clin Pharmacol* 2015; 80: 372–80.
- 36 Cook CD, Helliessen PJ, Agathon S. Relation between mechanics of respiration, lung size and body size from birth to young adulthood. *J Appl Physiol* 1958; 13: 349–52.
- 37 Perrie Y, Badhan RK, Kirby DJ, Lowry D, Mohammed AR, Ouyang D. The impact of ageing on the barriers to drug delivery. *J Control Release* 2012; 161: 389–98.
- 38 DeMeo DL, Weiss ST. Epidemiology. In: *Asthma and COPD: Basic Mechanisms and Clinical Management*, 2nd edn, eds Barnes PJ, Rennard SI, Drazen JM, Thomson NC. Amsterdam: Elsevier, 2009; 9–22.
- 39 Matsushima S, Matthews I, Woessner R, Pinault G, Hara H, Wilkins J, *et al.* Systemic pharmacokinetics of indacaterol, an inhaled once-daily long-acting beta2-agonist, in different ethnic populations. *Int J Clin Pharmacol Ther* 2012; 50: 545–56.
- 40 Shimada S, Vaidya S, Khindri S, Tashiro N, Cheng Y, Hara H, *et al.* Pharmacokinetics of QMF149 in Japanese versus Caucasian subjects: an open-label, randomized phase I study. *Int J Clin Pharmacol Ther* 2015; 53: 398–407.
- 41 Kim CS, Hu SC. Regional deposition of inhaled particles in human comparison between men and women. *J Appl Physiol* 1998; 84: 1834–44.
- 42 Allen A, Bal J, Cheesbrough A, Hamilton M, Kempford R. Pharmacokinetics and pharmacodynamics of intravenous and inhaled fluticasone furoate in healthy Caucasian and East Asian subjects. *Br J Clin Pharmacol* 2014; 77: 808–20.
- 43 James AL, Wenzel S. Clinical relevance of airway remodelling in airway diseases. *Eur Respir J* 2007; 30: 134–55.
- 44 Holgate ST. Airway remodeling. In: *Asthma and COPD: Basic Mechanisms and Clinical Management*, 2nd edn, eds Barnes PJ, Drazen JM, Rennard SI, Thomson NC. Amsterdam: Elsevier, 2009; 83–97.
- 45 Paredi P, Barnes PJ. The airway vasculature: recent advances and clinical implications. *Thorax* 2009; 64: 444–50.
- 46 Shaykhiev R, Otaki F, Bonsu P, Dang DT, Teater M, Strulovici-Barel Y, *et al.* Cigarette smoking reprograms apical junctional complex molecular architecture in the human airway epithelium *in vivo*. *Cell Mol Life Sci* 2011; 68: 877–92.

- 47 Sakagami M. Insulin disposition in the lung following oral inhalation in humans: a meta-analysis of its pharmacokinetics. *Clin Pharmacokinet* 2004; 43: 539–52.

Supporting Information

Additional Supporting Information may be found in the online version of this article at the publisher's web-site:

<http://onlinelibrary.wiley.com/doi/10.1111/bcp.12999/supinfo>.

Figure S1 Dose-normalized visual predictive checks (VPC) to evaluate model performance, separated by healthy volunteers, patients with asthma and patients with COPD. Binning was performed by number of data points per bin (before removal of concentrations below the LLOQ). Top: semi-logarithmic VPC for plasma concentrations plotted vs. time after dose; middle: VPC for plasma concentrations below the LLOQ plotted vs. time after dose; bottom: semi-logarithmic VPC for cumulative amount of olodaterol excreted into urine plotted vs. time after dose. Orange line: median of the observed data; blue dashed lines: 2.5th and 97.5th percentiles of the observed data; orange shaded boxes: 95% confidence interval around the median of the specific simulated data bin; blue shaded boxes: 95% confidence interval around the 2.5th and 97.5th percentile of the specific simulated data bins; grey points: measured concentrations/amounts; white filled points: 2.5th/median/97.5th percentile of the observed data at the median time point after dose of the specific bins. An additional VPC representing the plasma concentration–time profile from 0–12 after olodaterol inhalation can be found in Figure S4 of the online supplementary material

Figure S2 Standard goodness-of-fit plots for plasma PK data after olodaterol inhalation including a colour coding for healthy volunteers, patients with COPD and patients with asthma. Top left: logarithmic plot of olodaterol observations plotted vs. predictions; top right: logarithmic plot of observations plotted vs. individual predictions (both plots: predictions below the LLOQ have been removed); bottom left: semi-logarithmic plot of absolute individual weighted residuals plotted vs. individual predictions; bottom right: semi-logarithmic plot of conditional weighted residuals plotted vs. time after last dose. Black lines (upper plots): lines of identity; thin black lines: lower limit of quantification

Figure S3 Standard goodness-of-fit plots for urine data after olodaterol inhalation including a colour coding for healthy volunteers, patients with COPD and patients with asthma. Top left: logarithmic plot of olodaterol observations plotted vs. predictions, top right: logarithmic plot of observations plotted vs. individual predictions (both plots: predictions below the LLOQ have been removed); bottom left: semi-logarithmic plot of absolute individual weighted residuals plotted vs. individual predictions; bottom right: semi-logarithmic plot of conditional weighted residuals plotted vs. time after last dose. Black lines (upper plots): lines of identity; thin black lines: lower limit of quantification

Figure S4 Dose-normalized visual predictive checks (VPC) to evaluate model performance for healthy volunteers up to 24 h after olodaterol inhalation. Binning was performed by

number of data points per bin (before removal of concentrations below the LLOQ). Top: semi-logarithmic VPC for plasma concentrations plotted vs. time after dose; middle: VPC for plasma concentrations below the LLOQ plotted vs. time after dose; bottom: semi-logarithmic VPC for cumulative amount of olodaterol excreted into urine plotted vs. time after dose. Orange line: median of the observed data; blue dashed lines: 2.5th and 97.5th percentiles of the observed data; orange shaded boxes: 95% confidence interval around the median of the specific simulated data bin; blue shaded

boxes: 95% confidence interval around the 2.5th and 97.5th percentile of the specific simulated data bins; grey points: measured concentrations/amounts; white filled points: 2.5th/median/97.5th percentile of the observed data at the median time point after dose of the specific bins

Table S1 Influence of covariate effects on C_{max} , AUC_{plasma} and AUC_{Lung} including between subject and between occasion variability after single dose and at steady state (assumed after 14 inhaled doses of 5 μ g) including the 95% confidence interval ($n = 1000$ simulations per scenario)